



DYNAMIC STABILITY OF CURVED PANELS WITH CUTOUTS

S. K. SAHU AND P. K. DATTA

*Department of Aerospace Engineering, Indian Institute of Technology,
Kharagpur, At/P.O. Kharagpur-721302 (W.B.), India. E-mail: pkdatta@aero.iitkgp.ernet.in*

(Received 8 March 2001, and in final form 23 July 2001)

The parametric instability behaviour of curved panels with cutouts subjected to in-plane static and periodic compressive edge loadings are studied using finite element analysis. The first order shear deformation theory is used to model the curved panels, considering the effects of transverse shear deformation and rotary inertia. The theory used is the extension of dynamic, shear deformable theory according to Sanders' first approximation for doubly curved shells, which can be reduced to Love's and Donnell's theories by means of tracers. The effects of static and dynamic load factors, geometry, boundary conditions and the cutout parameters on the principal instability regions of curved panels with cutouts are studied in detail using Bolotin's method. Quantitative results are presented to show the effects of shell geometry and load parameters on the stability boundaries. Results for plates are also presented as special cases and are compared with those available in the literature.

© 2002 Elsevier Science Ltd.

1. INTRODUCTION

The structural elements subjected to in-plane periodic forces may lead to dynamic instability, due to certain combinations of the values of load parameters. The instability may occur below the critical load of the structure under compressive loads over a range or ranges of excitation frequencies. Several means of combating resonance such as damping and vibration isolation may be inadequate and sometimes dangerous with reverse results [1]. Cutouts are inevitable in aerospace, civil, mechanical and marine structures mainly for practical considerations. In aerospace structures, cutouts are commonly found as access ports for mechanical and electrical systems, or simply to reduce weight. Cutouts in wing spars and cover panels of commercial transport wings and military fighter wings are needed to provide access for hydraulic lines and for damage inspection. Cutouts are also made to lighten the loads, provide ventilation and for modifying the resonant frequency of the structures. In addition, the designers often need to incorporate cutouts or openings in a structure to serve as doors and windows. Thus the dynamic stability of structures with cutouts are of great technical importance for understanding the dynamic systems under periodic loads.

Despite the practical importance of these structures, the number of technical papers and reports dealing with the subjects are very limited due to the complexity involved. An extensive bibliography of earlier works on these problems are given in review papers [1–3] through 1987. The parametric instability characteristics of plates subjected to various types of loads was studied by Hutt and Salam [4]. Lee and Ng [5] studied the dynamic stability of plate on multiple line and point supports. Most of the investigators [6–8] studied the

dynamic stability of closed cylindrical shells with a simply supported boundary condition, using an analytical approach. The dynamic instability of conical shells was studied by Ng *et al.* [9] using Generalized Differential Quadrature method. The study of the parametric instability behaviour of curved panels is new. The dynamic stability of uniaxially loaded cylindrical panels with transverse shear effects is studied by Ng *et al.* [10]. The dynamic stability of laminated composite cylindrical shells were studied by Ng *et al.* [11], Ganapathi and Balamurugan [12] and many others. Previous investigations involving cutouts were mainly confined to free vibration of plates. A finite element analysis of a clamped plate with different cutout sizes, along with experiments using holographic interferometry, was carried out by Monahan *et al.* [13]. Paramsivam [14] used a finite difference approach in analyzing the effects of openings on the fundamental frequencies of plates with simply supported and clamped boundary conditions. The dynamic characteristics of rectangular plates with one or two cutouts using a finite difference formulation, based on variational principles were obtained by Aksu and Ali [15], along with experimental verifications. Ali and Atwal [16] studied the natural frequencies of simply supported rectangular plates and rectangular cutouts using the Rayleigh–Ritz method. The linear and large amplitude flexural vibration of isotropic and composite plates with cutout was studied by Reddy [17] using finite element method. Mundkur *et al.* [18] studied the vibration of square plates with square cutouts by using boundary characteristics orthogonal polynomials satisfying the boundary conditions. Chang and Chiang [19] studied the vibration of the rectangular plate with an interior cutout by using finite element method. Lam and Hung [20] investigated the flexural vibrations of plates with discontinuities in the form of cracks and cutouts using orthogonal polynomial functions, generated using the Gram Schmidt process. Lee *et al.* [21] predicted the natural frequencies of rectangular plates with an arbitrarily located rectangular cutout. Huang and Sakiyama [22] analyzed the free vibration of rectangular plates with variously shaped holes. Rossi [23] has dealt with the frequency of transverse vibrations of the structural systems, especially with the fixed boundaries. Young *et al.* [24] presented the free vibration of thick rectangular plates with depression, grooves or cutouts using three-dimensional (3-D) elasticity and Ritz method. Ritchie and Rhodes [25] have investigated theoretically and experimentally the behaviour of simply supported uniformly compressed rectangular plates with central holes, using a combination of Rayleigh–Ritz and finite element methods. The buckling of rectangular plates with central cutouts are investigated by Ko [26] using structural performance and resizing (SPAR) finite element computer program. Brogan *et al.* [27] presented analytical and experimental investigations of the dynamic behaviour of closed circular cylindrical shell with a rectangular cutout. Toda and Komatsu [28] studied analytically and experimentally the effect of circular cutouts on the resonant frequencies of thin cylindrical shells using simplified Rayleigh–Ritz type approximations. The effects of cutouts on the natural frequencies of curved panels have been treated sparsely in the literature. Liew and Lim [29] examined the natural frequencies and vibratory characteristics of shallow shells having an outer super-elliptical periphery and an inner super-elliptical cutout using the Ritz procedure. The free vibration characteristics of unstiffened [30] and longitudinally stiffened [31] square panels with symmetrical square cutouts are investigated by Sivasubramonian *et al.* using finite element method. To the best of the authors' knowledge, there is no study involving dynamic stability of curved panel with a cutout. The application of a cutout on the structural component will alter the global quantities such as stresses, free vibration frequency, buckling load and dynamic instability region (DIR).

In the present study, the dynamic stability of curved panels with cutouts are investigated. The influences of various parameters like effects of static and dynamic load factors, size of

cutout, geometry and various boundary conditions on the instability behaviour of curved panels have been examined. The present formulation of the problem is made general to accommodate a doubly curved panel with finite curvatures in both the directions having arbitrary load and boundary conditions.

2. THEORY AND FORMULATIONS

The basic configuration of the problem considered here is a doubly curved panel with cutout as shown in Figure 1, subjected to harmonic in-plane edge loading.

2.1. GOVERNING EQUATIONS

The equation of equilibrium for free vibration of a shear deformable doubly curved panel with cutout subjected to in-plane external loading can be written as:

$$\begin{aligned} \frac{\partial N_x}{\partial x} + \frac{\partial N_{xy}}{\partial y} - \frac{1}{2}C_2\left(\frac{1}{R_y} - \frac{1}{R_x}\right)\frac{\partial M_{xy}}{\partial y} + C_1\frac{Q_x}{R_x} + C_1\frac{Q_y}{R_{xy}} &= \rho h \frac{\partial^2 u}{\partial t^2}, \\ \frac{\partial N_{xy}}{\partial x} + \frac{\partial N_y}{\partial y} + \frac{1}{2}C_2\left(\frac{1}{R_y} - \frac{1}{R_x}\right)\frac{\partial M_{xy}}{\partial x} + C_1\frac{Q_y}{R_y} + C_1\frac{Q_x}{R_{xy}} &= \rho h \frac{\partial^2 v}{\partial t^2}, \\ \frac{\partial Q_x}{\partial x} + \frac{\partial Q_y}{\partial y} - \frac{N_x}{R_x} - \frac{N_y}{R_y} - 2\frac{N_{xy}}{R_{xy}} + N_x^0\frac{\partial^2 w}{\partial x^2} + N_y^0\frac{\partial^2 w}{\partial y^2} &= \rho h \frac{\partial^2 w}{\partial t^2}, \\ \frac{\partial M_x}{\partial x} + \frac{\partial M_{xy}}{\partial y} - Q_x &= \frac{\rho h^3}{12} \frac{\partial^2 \theta_x}{\partial t^2}, \\ \frac{\partial M_{xy}}{\partial x} + \frac{\partial M_y}{\partial y} - Q_y &= \frac{\rho h^3}{12} \frac{\partial^2 \theta_y}{\partial t^2}, \end{aligned} \tag{1}$$

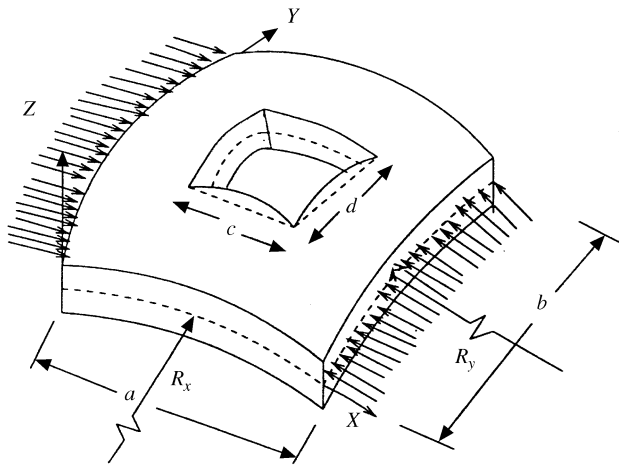


Figure 1. Geometry and co-ordinate systems of a doubly curved panel with cutout.

where N_x^0 and N_y^0 are the external loading in X and Y directions respectively. C_1 and C_2 are tracers by which the analysis can be reduced to that of Sanders', Love's and Donnell's theories. If the tracer coefficients $C_1 = C_2 = 1$, the equation corresponds to the generalization of Sanders' first approximation theory. The case $C_1 = 1, C_2 = 0$ correspond to Love's theories of thin shells generalized to include shear deformations. Finally, if $C_1 = C_2 = 0$, the equation is reduced to a shear deformable version of Donnell's theories. The constants R_x, R_y and R_{xy} identify the radii of curvature in the X, Y directions and the radius of twist. The equation of motion can be written in matrix form as

$$[M]\{\ddot{q}\} + [[K_e] - \lambda[K_g]]\{q\} = 0. \tag{2}$$

The in-plane load $N(t)$ is periodic and can be expressed in the form

$$N(t) = N_s + N_t \cos \Omega t, \tag{3}$$

where N_s is the static portion of $N(t)$. N_t is the amplitude of the dynamic portion of $N(t)$ and Ω is the frequency of excitation. The static buckling load of the panel N_{cr} is the measure of the magnitude of N_s and N_t ,

$$N_s = \alpha N_{cr}, \quad N_t = \beta N_{cr}, \tag{4}$$

where α and β are termed as static and dynamic load factors respectively. Using equation (3), the equation of motion is obtained as

$$[M]\{\ddot{q}\} + [[K_e] - \alpha N_{cr}[K_g] - \beta N_{cr}[K_g] \cos \Omega t]\{q\} = 0. \tag{5}$$

Equation (5) represents a system of second order differential equations with periodic coefficients of the Mathieu–Hill type. The development of regions of instability arises from Floquet's theory which establishes the existence of periodic solutions. The boundaries of the dynamic instability regions are formed by the periodic solutions of period T and $2T$, where $T = 2\pi/\Omega$. The boundaries of the primary instability regions with period $2T$ are of practical importance [32] and the solution can be achieved in the form of the trigonometric series

$$q(t) = \sum_{k=1,3,5}^{\infty} \left[\{a_k\} \sin \frac{k\Omega t}{2} + \{b_k\} \cos \frac{k\Omega t}{2} \right]. \tag{6}$$

Putting this in equation (5) and if only the first term of the series is considered, equating coefficients of $\sin \Omega t/2$ and $\cos \Omega t/2$, equation (5) reduces to

$$\left[[K_e] - \alpha N_{cr}[K_g] \pm \frac{1}{2} \beta N_{cr}[K_g] - \frac{\Omega^2}{4}[M] \right] \{q\} = 0. \tag{7}$$

Equation (7) represents an eigenvalue problem for known values of α, β and N_{cr} . The two conditions under a plus and minus sign correspond to two boundaries of the dynamic instability region. The eigenvalues are Ω , which give the boundary frequencies of the instability regions for given values of α and β . In this analysis, the computed static buckling load of the panel is considered as the reference load in line with Moorthy *et al.* [33] and Ganapathi *et al.* [34].

The eight-node curved isoparametric quadratic element is employed in the present analysis with five degrees of freedom (d.o.f.) u, v, w, θ_x and θ_y per node. First order shear deformation theory (FSDT) is used and the shear correction coefficient has been employed to account for the non-linear distribution of the shear strains through the thickness. The

displacement field assumes that mid-plane normal remains straight but not necessarily normal after deformation, so that

$$\bar{u}(x, y, z) = u(x, y) + z\theta_x(x, y), \quad \bar{v}(x, y, z) = v(x, y) + z\theta_y(x, y), \quad \bar{w}(x, y, z) = w(x, y), \quad (8)$$

where θ_x, θ_y are the rotations of the mid-surface. Also, $\bar{u}, \bar{v}, \bar{w}$ and u, v, w are the displacement components in the x, y, z directions at any section and at mid-surface respectively. The constitutive relationships for the shell are given by

$$F = [D]\{\varepsilon\}, \quad (9)$$

where

$$F = [N_x, N_y, N_{xy}, M_x, M_y, M_{xy}, Q_x, Q_y]^T, \quad (10)$$

$$[D] = \begin{bmatrix} \frac{Eh}{1-\nu^2} & \frac{\nu Eh}{1-\nu^2} & 0 & 0 & 0 & 0 & 0 & 0 \\ \frac{\nu Eh}{1-\nu^2} & \frac{Eh}{1-\nu^2} & 0 & 0 & 0 & 0 & 0 & 0 \\ 0 & 0 & \frac{Eh}{2(1+\nu)} & 0 & 0 & 0 & 0 & 0 \\ 0 & 0 & 0 & \frac{Eh^3}{12(1-\nu^2)} & \frac{\nu Eh^3}{12(1-\nu^2)} & 0 & 0 & 0 \\ 0 & 0 & 0 & \frac{Eh^3\nu}{12(1-\nu^2)} & \frac{Eh^3}{12(1-\nu^2)} & 0 & 0 & 0 \\ 0 & 0 & 0 & 0 & 0 & \frac{Eh^3}{24(1+\nu)} & 0 & 0 \\ 0 & 0 & 0 & 0 & 0 & 0 & \frac{Eh}{2\cdot4(1+\nu)} & 0 \\ 0 & 0 & 0 & 0 & 0 & 0 & 0 & \frac{Eh}{2\cdot4(1+\nu)} \end{bmatrix} \quad (11)$$

and

$$\{\varepsilon\} = \{\varepsilon_l\} + \{\varepsilon_{nl}\}. \quad (12)$$

Reissner’s shear correction factor of 5/6 is included for all numerical computations. Extensions of shear deformable Sanders’ kinematic relations for doubly curved shells [35, 36] are used in the analysis. The linear strain displacement relations are

$$\begin{aligned} \varepsilon_{xl} &= \frac{\partial u}{\partial x} + \frac{w}{R_x} + z\kappa_x, & \varepsilon_{yl} &= \frac{\partial v}{\partial y} + \frac{w}{R_y} + z\kappa_y, & \gamma_{xyl} &= \frac{\partial u}{\partial y} + \frac{\partial v}{\partial x} + z\kappa_{xy}, \\ \gamma_{yz} &= \frac{\partial w}{\partial y} + \theta_y - C_1 \frac{v}{R_y}, & \gamma_{xz} &= \frac{\partial w}{\partial x} + \theta_x - C_1 \frac{u}{R_x}. \end{aligned} \quad (13)$$

where

$$\kappa_x = \frac{\partial \theta_x}{\partial x}, \quad \kappa_y = \frac{\partial \theta_y}{\partial y}, \quad \kappa_{xy} = \frac{\partial \theta_x}{\partial y} + \frac{\partial \theta_y}{\partial x} + \frac{1}{2}C_2 \left(\frac{1}{R_y} - \frac{1}{R_x} \right) \left(\frac{\partial v}{\partial x} - \frac{\partial u}{\partial y} \right). \quad (14)$$

The element geometric stiffness matrix for the doubly curved panel is derived using the non-linear strain components as

$$\begin{aligned}\varepsilon_{xnl} &= \frac{1}{2}\left(\frac{\partial u}{\partial x}\right)^2 + \frac{1}{2}\left(\frac{\partial v}{\partial x}\right)^2 + \frac{1}{2}\left(\frac{\partial w}{\partial x} - \frac{u}{R_x}\right)^2 + \frac{1}{2}z^2\left[\left(\frac{\partial\theta_x}{\partial x}\right)^2 + \left(\frac{\partial\theta_y}{\partial x}\right)^2\right], \\ \varepsilon_{ynl} &= \frac{1}{2}\left(\frac{\partial u}{\partial y}\right)^2 + \frac{1}{2}\left(\frac{\partial v}{\partial y}\right)^2 + \frac{1}{2}\left(\frac{\partial w}{\partial y} - \frac{v}{R_y}\right)^2 + \frac{1}{2}z^2\left[\left(\frac{\partial\theta_x}{\partial y}\right)^2 + \left(\frac{\partial\theta_y}{\partial y}\right)^2\right], \\ \gamma_{xynl} &= \left[\left(\frac{\partial u}{\partial x}\right)\frac{\partial u}{\partial y} + \frac{\partial v}{\partial x}\left(\frac{\partial v}{\partial y}\right) + \left(\frac{\partial w}{\partial x} - \frac{u}{R_x}\right)\left(\frac{\partial w}{\partial y} - \frac{v}{R_y}\right)\right] \\ &\quad + z^2\left[\left(\frac{\partial\theta_x}{\partial x}\right)\left(\frac{\partial\theta_x}{\partial y}\right) + \left(\frac{\partial\theta_y}{\partial x}\right)\left(\frac{\partial\theta_y}{\partial y}\right)\right].\end{aligned}\quad (15)$$

The element matrices are derived as

Elastic stiffness matrix

$$[k_e]_e = \int [B]^T [D] [B] dx dy. \quad (16)$$

Geometric stiffness matrix

$$[k_g]_e = \int [G]^T [S] [G] dv. \quad (17)$$

Consistent mass matrix

$$[m]_e = \int [N]^T [I] [N] dx dy \quad (18)$$

The overall matrices $[K_e]$, $[K_g]$ and $[M]$ are obtained by assembling the corresponding element matrices.

2.2. COMPUTER PROGRAM

A computer program has been developed to perform all the necessary computations. Element elastic stiffness matrices and mass matrices are obtained using a standard procedure. The geometric stiffness matrix is essentially a function of the in-plane stress distribution in the element due to applied edge loadings. Since the stress field is non-uniform, due to cutout, plane stress analysis is carried out using the finite element method to determine the stresses and these are used to formulate the geometric stiffness matrix. Reduced integration technique is adopted in order to avoid possible shear locking. Element matrices are assembled into global matrices, using skyline technique. Subspace iteration method is adopted throughout to solve the eigenvalue problems.

3. RESULTS AND DISCUSSIONS

The convergence studies have been carried out for fundamental frequencies of vibration of the SSSS square plates with a square hole of size ratio $c/a = 0.5$, for different mesh

TABLE 1

Convergence of non-dimensional fundamental frequencies of an SSSS square plate with a hole of size ratio $c/a = 0.5$. $a/b = 1, b/h = 100; \nu = 0.3$; non-dimensional frequency, $\omega = \bar{\omega}a^2\sqrt{(\rho h/D)}$

Mesh division	Non-dimensional frequencies			
	1	2	3	4
8 × 8	23.570	40.5227	40.5227	72.2728
12 × 12	23.4703	40.1072	40.1072	71.4209
16 × 16	23.4364	39.9793	39.9793	71.1964
20 × 20	23.4218	39.9287	39.9287	71.1090
Reference [21]	(23.329)	39.712	39.712	(71.263)

TABLE 2

Comparison of non-dimensional fundamental frequencies of a simply supported SSSS square plate with a cutout. $a/b = 1, b/h = 100, \nu = 0.3$; non-dimensional frequency, $\omega = \bar{\omega}a^2\sqrt{(\rho h/D)}$

c/a	Non-dimensional frequencies					
	Present	PACFAC [20]	Reference [21]	Reference [20]	Reference [18]	Reference [37]
0	19.7336	19.752	19.739	19.740	19.7392	19.57
0.2	19.1339	19.120	18.901	18.762	20.1933	19.16
0.4	20.7387	20.732	20.556	20.785	—	—
0.5	23.4218	23.235	23.329	23.664	24.243	23.650
0.6	28.3068	28.241	28.491	28.844	—	—
0.8	56.9487	57.452	58.847	58.062	58.3585	58.25

divisions. As shown in Table 1, the frequencies of vibration are computed and the results are compared with the values by Lee *et al.* [21]. It shows the sufficient accuracy of the numerical solutions by the present method. From the above convergence study, 20 × 20 mesh has been employed to idealize the panel in the subsequent analysis. In order to investigate the accuracy and efficiency of the present formulation, the frequency parameters of plates with different cutout sizes are compared with the results using the package PACFAC 75 [20], the orthogonal polynomial functions by Lam and Hung [20], the numerical method based on Rayleigh quotient by Lee *et al.* [21], boundary characteristics orthogonal polynomials functions in the Rayleigh–Ritz method by Mundkar *et al.* [18], and that of Koushal and Bhat [37]; which are presented in Table 2. Good agreement exists for the present finite element results with those available in the literature. The present formulation is then validated for buckling of plate with cutout with the graphical results using the structural performance and resizing (SPAR) finite element computer program by Ko [26]. As seen from Figure 2, good agreement exists between both the finite element results. To validate the formulation further, the free vibration frequency parameters with computational results for clamped (CCCC) curved panel having cutout are compared with the work carried out by Sivasubramonian *et al.* [31]. The results are shown in Table 3. The above studies indicate good agreement between the present study and those from the literature. Once the free vibration and buckling results are validated, the dynamic instability studies are carried out.

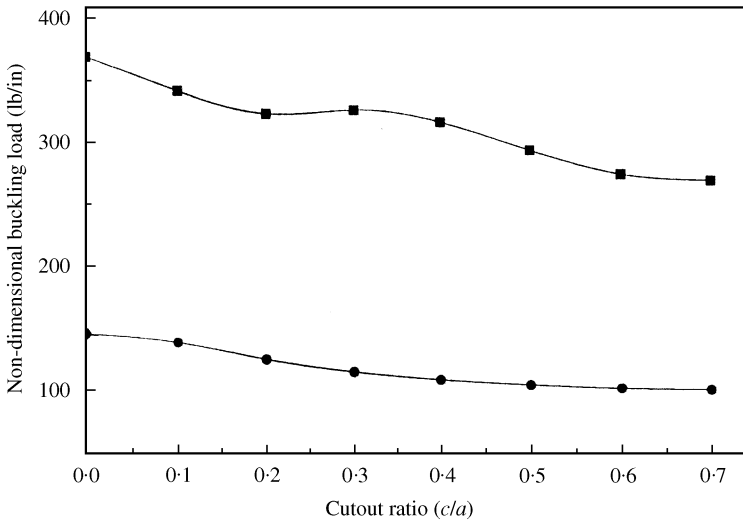


Figure 2. Comparison of buckling loads of plates with different sizes of cutouts: (●) SSSS (reference [26]); (■) CCCC (reference [26]); (—) Present work.

TABLE 3

Comparison of frequencies in Hz for the CCCC cylindrical curved panel with and without cutout. $a = b = 500 \text{ mm}$, $h = 2 \text{ mm}$, $\nu = 0.3$, $E = 7020 \text{ kg/mm}^2$, $\rho = 2720 \text{ kg/m}^3$

R	Mode no	c/a = 0.0		c/a = 0.5	
		Present FEM	Reference [31]	Present FEM	Reference [31]
Plate	1	69.76	69.2	126.73	125.7
	2	142.27	140.9	147.92	147.3
	3	142.27	140.9	147.92	147.3
	4	209.79	206.9	199.04	199.2
2000	1	215.23	213.9	184.73	185.3
	2	245.23	243.2	187.52	188.2
	3	328.34	326.1	295.68	295.9
	4	336.83	333.3	310.30	309.7

3.1. DYNAMIC STABILITY STUDIES

The DIR are plotted for a flat and cylindrical panel with/without static component to consider the effects of static load factor, size of cutout, different panel geometry and boundary conditions. A simply supported plate of dimensions $a = b = 500 \text{ mm}$, $h = 5 \text{ mm}$, $E = 70 \text{ Gpa}$, $\nu = 0.3$, $\rho = 2800 \text{ kg/m}^3$ is described as a standard case and the computed buckling load of this panel is taken as the reference load in line with Moorthy *et al.* [33]. The non-dimensional excitation frequency $\Omega = \bar{\Omega}a^2\sqrt{\rho h/D}$ is used throughout the dynamic instability studies (unless otherwise mentioned), where $\bar{\Omega}$ is the excitation frequency in rad/s, $D = Eh^3/12(1 - \nu^2)$. For a given panel, the effect of size of cutout on the instability region are studied from 0.0 (no cutout) to 0.8 at an interval of 0.1. However, for clarity, the plots are shown for size of cutout 0.0 (no cutout) to 0.8 at an interval of 0.2 and $c/a = 0.5$ and are presented in Figure 3. The results of plates with cutout ratio $c/a = 0.0$ is compared with

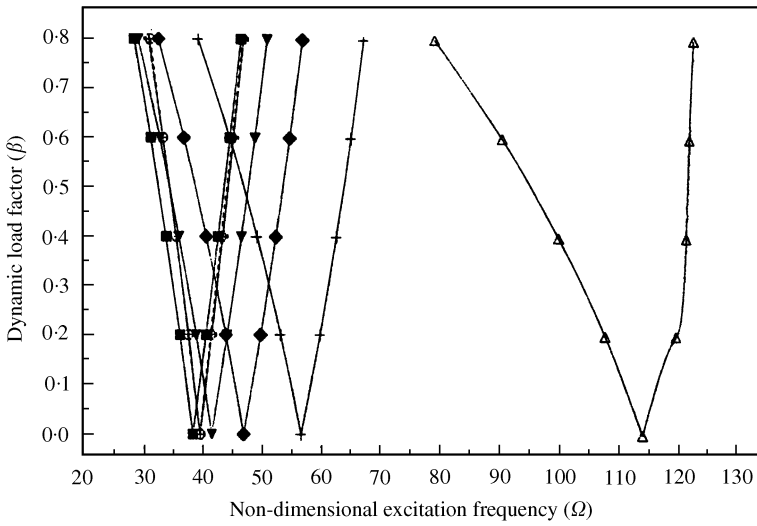


Figure 3. Effect of size of cutout on instability region of the simply supported plate for $c/a = \dots, 0.0$ (reference [4]); $\circ, 0.0$; $\blacksquare, 0.2$; $\blacktriangledown, 0.4$; $\blacklozenge, 0.5$; $+, 0.6$ and $\triangle, 0.8$; $a/R_x = 0, b/R_y = 0.0, \alpha = 0.0$.

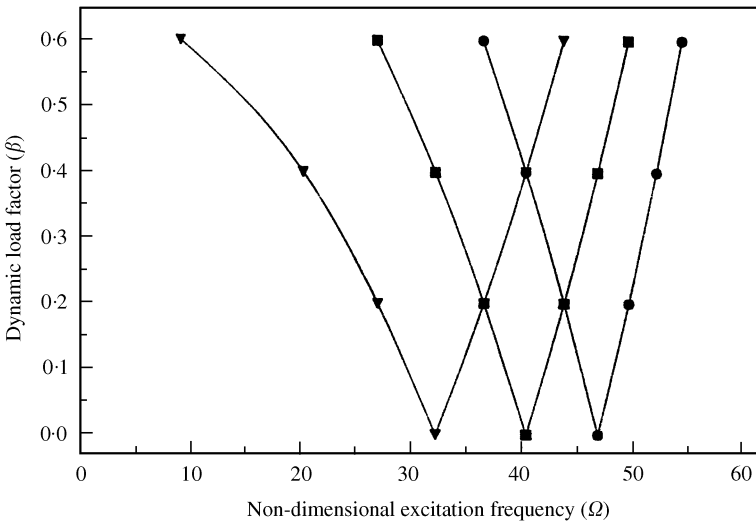


Figure 4. Effect of static load factor on instability region of the simply supported plate with cutout: $a/b = 1, a/R_x = 0.0, b/R_y = 0.0, c/a = 0.5$ for $\alpha = \bullet, 0.0$; $\blacksquare, 0.2$ and $\blacktriangledown, 0.4$.

those of Hutt and Salam [4], which is in close agreement. With the introduction of cutout, it can be observed that, the onset of instability occurs with lower excitation frequencies for small cutouts in simply supported plates up to $c/a = 0.2$. With an increase of cutout size, the onset of excitation frequency increases along with wider dynamic instability regions. The onset of instability occurs with higher excitation frequency for plates with cutout size of $c/a = 0.4$ onwards than those without cutout ($c/a = 0.0$). The onset of instability occurs at a higher excitation frequencies up to plates with cutout of $c/a = 0.8$ with wider instability regions. This may be attributed to the predominance of the boundary restraints over the entire plate. The effect of static component of load on the instability regions of the plate with a cutout of size $c/a = 0.5$ is studied for $\alpha = 0.0, 0.2$ and 0.4 , as shown in Figure 4. Due to an

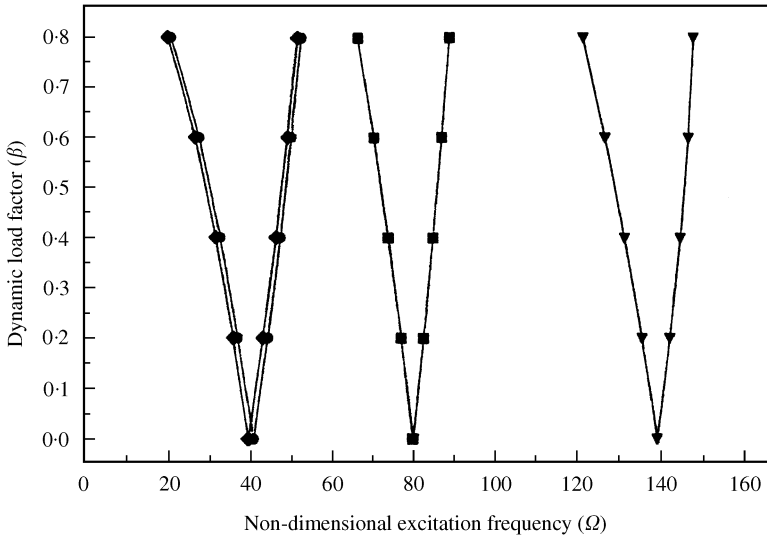


Figure 5. Effect of cutout on instability region of different curved panels: flat panel ($a/R_x = b/R_y = 0$), cylindrical ($a/R_x = 0, b/R_y = 0.25$), spherical ($a/R_x = b/R_y = 0.25$), hyperbolic paraboloid ($a/R_x = -0.25, b/R_y = 0.25$) for $a/b = 1, c/a = 0.5$ and $\alpha = 0.2$. geometry: ●, plate; ■, cylindrical; ▼, spherical; ◆, hyperbolic paraboloid.

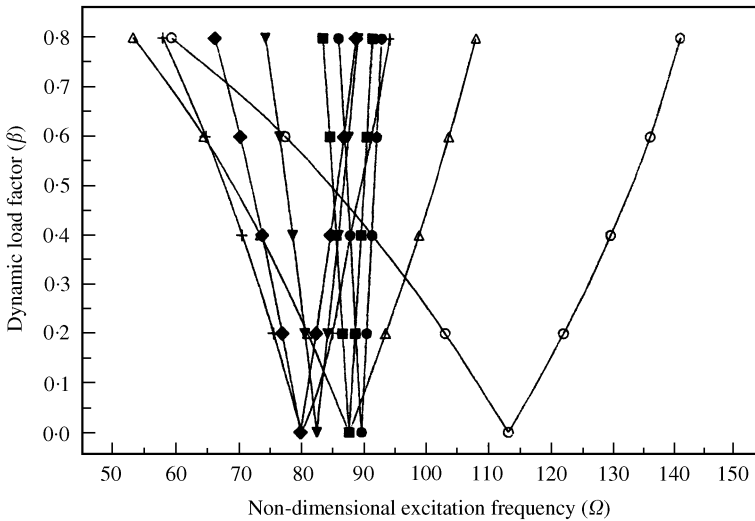


Figure 6. Effect of size of cutout on instability region of the simply supported cylindrical panel for $c/a =$ ●, 0.0; ■, 0.2; ▼, 0.4; ◆, 0.5; +, 0.6; △, 0.7 and ○, 0.8; $a/R_x = 0, b/R_y = 0.25, \alpha = 0.2$.

increase of static component, the instability regions tend to shift to lower frequencies and become wider. All further studies are carried out with a static load factor of 0.2 (unless otherwise mentioned). Studies have also been made for the comparison of instability regions for different shell geometries. The dynamic instability regions are plotted for plate and different curved panels such as cylindrical ($b/R_y = 0.25$), spherical ($a/R_x = b/R_y = 0.25$) and hyperbolic paraboloids ($a/R_x = -0.25, b/R_y = 0.25$) with cutouts of $c/a = 0.5$ and are compared in Figure 5. It is observed, that the excitation frequency increases with the introduction of curvatures from the plate to curved panels with cutout. However, the

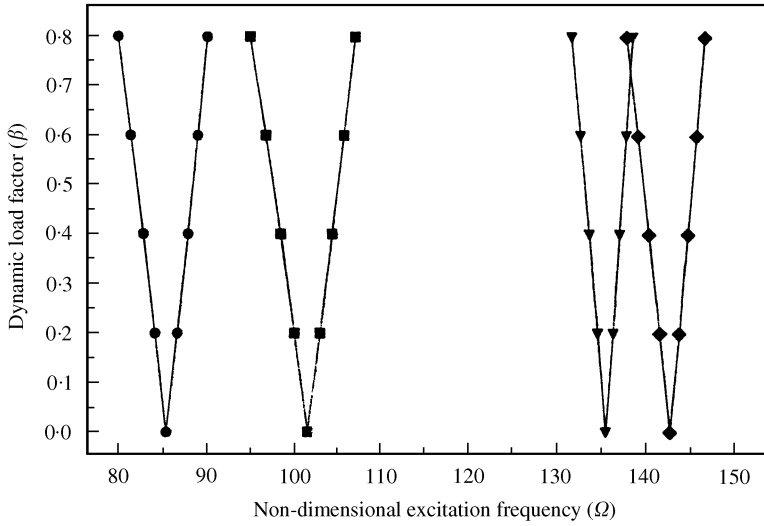


Figure 7. Effect of boundary conditions (●, SSSS; ■, CSCS; ▼, SCSC; ◆, CCCC) on instability region of the curved panel for $a/b = 1$, $a/R_x = 0.0$, $b/R_y = 0.25$, $c/a = 0.3$ and $\alpha = 0.2$.

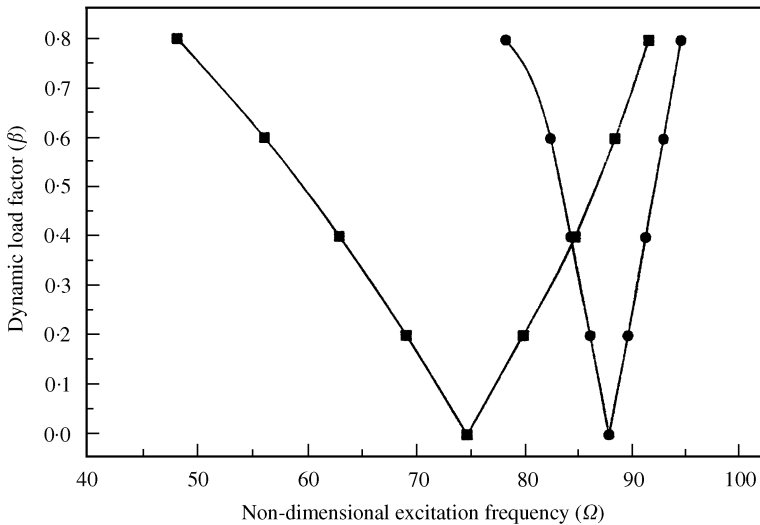


Figure 8. Effect of cutout on instability region of the curved panel subjected to biaxial loading for $a/b = 1$, $\alpha = 0.2$ and $c/a = \bullet, 0.0$ and $\blacksquare, 0.5$.

hyperbolic paraboloid with cutout shows similar instability behaviour as that of a flat panel with no stiffness being added due to the curvature of the panel with cutout. Similar observations were also obtained by Leissa and Kadi [38] on a study of free vibration of shells, especially on a supported platform. The effect of size of cutout on instability regions of a simply supported cylindrical panel is investigated for $c/a = 0.0, 0.2, 0.4, 0.5, 0.6$ and 0.8 . As shown in Figure 6, the onset of instability occurs earlier with an increase of size of cutout up to $c/a = 0.5$. With further increase of cutout, the excitation frequency gradually increases having wider dynamic instability regions. The onset of instability occurs with higher excitation frequency for the cylindrical panel with cutout size $c/a = 0.8$ than that without cutout with very wide dynamic instability region. The onset of instability will even occur

earlier for a cylindrical panel with cutout $c/a = 0.8$ for a higher value of dynamic load beyond $\beta = 0.6$. Figure 7 shows the influence of different boundaries (SSSS, SCSC, CSCS, CCCC) on the principal instability regions. As expected, the instability occurs at a higher excitation frequency from simply supported to clamped edges due to the restraint at the edges. The width of the instability regions also decreased with the increase of restraint at the edges. The study is then extended to dynamic stability of a cylindrical panel with cutout subjected to biaxial loading. The instability regions are plotted for the cylindrical panel with cutout $c/a = 0.5$ and compared with that of the panel without cutout. As shown in Figure 8, the instability appears at a lower excitation frequency with increasing dynamic instability region for biaxial loading of cylindrical panel with cutout.

4. CONCLUSION

The results of the stability studies of the plates and shells with cutout can be summarized as follows:

1. The onset of instability occurs at lower excitation frequencies with increase of cutout size in plates with wider instability regions. With further increase of size of cutout, the excitation frequency increases and is sometimes higher than that of the plate without cutout.
2. Due to static component, the instability regions tend to shift to lower frequencies with wide instability regions showing destabilizing effect on the dynamic stability behaviour of the curved panel with cutout.
3. The effect of curvature is reduced with increase of size of cutout.
4. The curved panels with cutout show more stiffness with the addition of curvatures. But the hyperbolic paraboloid panels, especially on a supported platform, behave like a plate with no stiffness being added due to the curvature of the shell.
5. The instability regions have been influenced due to restraint provided at the edges of the curved panel with cutout. The predominance of the boundary restraints may be responsible for increase of excitation frequencies, especially for plate and curved panels with higher size of cutout. The onset of instability occurs for curved panels with restraints at the straight edges than that of curved boundary.
6. It was observed that instability appears at lower excitation frequency with increasing dynamic instability region for cylindrical panel with cutout, subjected to biaxial loading.

REFERENCES

1. R. M. EVAN-IWANOWSKI 1965 *Applied Mechanics Review* **18**, 699–702. On the parametric response of structures.
2. R. A. IBRAHIM 1978 *Shock and Vibration Digest* **10**, 41–57. Parametric vibration part III. Current problems (1).
3. G. J. SIMITSES 1987 *Appl. Mechanics Review* 1403–1408. Instability of dynamically loaded structures.
4. J. M. HUTT and A. E. SALAM 1971 *American Society of Civil Engineers Journal of Engineering Mechanics* **3**, 879–899 Dynamic instability of plates by finite element.
5. H. P. LEE and T. Y. NG 1995 *Journal of Sound and Vibration* **185**, 345–356. Dynamic stability of a plate on multiple line and point supports subjected to pulsating conservative in-plane loads.
6. K. Y. LAM and T. Y. NG 1997 *Journal of Sound and Vibration* **207**, 497–520. Dynamic stability of cylindrical shells subjected to conservative periodic axial loads using different shell theories.
7. K. Y. LAM and T. Y. NG 1999 *American Institute of Aeronautics and Astronautics Journal* **37**, 137–140. Parametric resonance of cylindrical shells by different shell theories.

8. T. Y. NG, K. Y. LAM and J. N. REDDY 1998 *Journal of Sound and Vibration* **214**, 513–529. Parametric resonance of a rotating cylindrical shell subjected to periodic axial load.
9. T. Y. NG, L. I. HUA, K. Y. LAM and C. T. LOY 1999 *International Journal for Numerical Methods in Engineering* **44**, 819–837. Parametric instability of conical shells by the Generalized Differential Quadrature method.
10. T. Y. NG, K. Y. LAM and J. N. REDDY 1999 *International Journal of Solids and Structures* **36**, 3483–3496. Dynamic stability of cylindrical panels with transverse shear effects.
11. T. Y. NG, K. Y. LAM and J. N. REDDY 1998 *International Journal of Mechanical Sciences* **40**, 805–823. Dynamic stability of cross-ply laminated composite cylindrical shells.
12. M. GANAPATHI and V. BALAMURUGAN 1998 *Computers and Structures* **69**, 181–189. Dynamic instability analysis of a laminated composite circular cylindrical shell.
13. J. MONAHAN, P. J. NEMERGUT and G. E. MADDUX 1970 *The Shock and Vibration Bulletin* **41**, 37–49. Natural frequencies and mode shapes of plates with interior cutouts.
14. P. PARAMSIVAM 1973 *Journal of Sound and Vibration* **30**, 173–178. Free vibration of square plates with square openings.
15. G. AKSU and R. ALI 1976 *Journal of Sound and Vibration* **44**, 147–158. Determination of dynamic characteristics of rectangular plates with cutouts using a finite difference formulation.
16. R. ALI and S. J. ATWAL 1980 *Computers and Structures* **12**, 819–823. Prediction of natural frequencies of vibration of rectangular plates with rectangular cutouts.
17. J. N. REDDY 1982 *Journal of Sound and Vibration* **83**, 1–10. Large amplitude flexural vibration of layered composite plates with cutout.
18. G. MUNDKUR, R. B. BHAT and S. NERIYA 1994 *Journal of Sound and Vibration* **176**, 136–144. Vibration of plates with cutouts using boundary characteristics orthogonal polynomial functions in the Rayleigh–Ritz method.
19. C. N. CHANG and F. K. CHIANG 1988 *Journal of Sound and Vibration* **125**, 477–486. Vibration analysis of a thick plate with an interior cutout by a finite element method.
20. K. Y. LAM and K. C. HUNG 1990 *Computers and Structures* **34**, 827–834. Orthogonal polynomials and subsectioning method for vibration of plates.
21. H. P. LEE, S. P. LIM and S. T. CHOW 1990 *Computers and Structures* **36**, 861–869. Prediction of natural frequencies of rectangular plates with rectangular cutouts.
22. M. HUANG and T. SAKIYAMA 1999 *Journal of Sound and Vibration* **226**, 769–786. Free vibration analysis of rectangular plates with variously shaped holes.
23. R. E. ROSSI 1999 *Journal of Sound and Vibration* **221**, 733–736. Transverse vibrations of thin, orthotropic rectangular plates with rectangular cutouts with fixed boundaries.
24. P. G. YOUNG, J. YUAN and S. M. DICKINSON 1996 *American Society of Mechanical Engineers Journal of Vibration and Acoustics* **118**, 184–189. Three dimensional analysis of the free vibration of thick rectangular plates with depressions, grooves or cutouts.
25. D. RITCHIE and J. RHODES 1975 *Aeronautical Quarterly* **xxiv**, 281–296. Buckling and post-buckling behaviour of plates with holes.
26. W. L. KO 1998 *NASA Technical Memorandum* **206542**, 1–47. Mechanical and thermal buckling behaviour of rectangular plates with different central cutout.
27. F. BROGAN, K. FORSEBERG and S. SMITH 1969 *American Institute of Aeronautics and Astronautics Journal* **7**, 903–911. Dynamic behaviour of a cylinder with a cutout.
28. S. TODA and K. KOMATSU 1977 *Journal of Sound and Vibration* **52**, 497–510. Vibration of circular cylindrical shells with cutouts.
29. K. M. LIEW and C. W. LIM 1994 *International Journal of Solids and Structures* **31**, 1519–1536. Vibration of perforated doubly curved shallow shells with rounded corners.
30. B. SIVASUBRAMONIAN, A. M. KULKARNI and G. V. RAO 1997 *Journal of Sound and Vibration* **200**, 227–234. Free vibration of curved panels with cutouts.
31. B. SIVASUBRAMONIAN, G. V. RAO and A. KRISHNAN 1999 *Journal of Sound and Vibration* **226**, 41–55. Free vibration of longitudinally stiffened curved panels with cutouts.
32. V. V. BOLOTIN 1964 *The Dynamic Stability of Elastic Systems*. San Francisco, CA: Holden-Day.
33. J. MOORTHY, J. N. REDDY J. N. and R. H. PLAUT 1990 *International Journals of Solids and Structures* **26**, 801–811. Parametric instability of laminated composite plates with transverse shear deformation.
34. M. GANAPATHI, P. BOISSE and D. SOLAUT 1999 *International Journal for Numerical Methods in Engineering* **46**, 943–956. Non-linear dynamic stability analysis of composite laminates under periodic in-plane loads.
35. J. N. REDDY 1984 *Journal of Engineering Mechanics, American Society of Civil Engineers* **110**, 794–809. Exact solutions of moderately thick laminated shells.

36. K. CHANDRASHEKHARA 1989 *Computers and Structures* **33**, 435–440. Free vibrations of anisotropic laminated doubly curved shells.
37. A. KOUSHAL and R. B. BHAT 1993 *Proceedings of Canadian Congress of Applied Mechanics, CANCAM '93, Ontario*. A comparison study of vibration of plate with cutouts using the finite element and Rayleigh–Ritz methods.
38. A. W. LEISSA and A. S. KADI 1971 *Journal of Sound and Vibration* **16**, 173–187. Curvature effects on shallow shell vibration.

APPENDIX A: NOMENCLATURE

a, b	dimensions of shell
R_x, R_y	radii of curvatures
c, d	dimensions of the cutout
E	Young's modulus
G	shear modulus
$[K]$	stiffness matrix
$[K_g]$	geometric stiffness matrix
$[M]$	mass matrix
N_{cr}	critical buckling load
$\{q\}$	vector of generalized co-ordinates
w	deflection of mid-plane of shell
ν	the Poisson ratio
ρ	mass density
θ_x, θ_y	rotations about axes
Ω, ω	frequency of forcing function and transverse vibration
α, β	static and dynamic load factors